RESEARCH ARTICLES

Effects of the India–Pakistan border earthquake on the atmospherics at 6 kHz and 9 kHz recorded at Tripura

Syam Sundar De[1,*], Barin Kumar De[2], Bijoy Bandyopadhyay[1], Suman Paul[1], Dilip Kumar Haldar[1], Adhip Bhowmick[2], Sudarsan Barui[1], Rousan Ali[2]

[1] *S. K. Mitra Centre for Research in Space Environment, Institute of Radio Physics and Electronics, University of Calcutta, Kolkata, India*

[2] *Tripura University, Department of Physics, Tripura, India*

Article history
Received August 17, 2010; accepted December 4, 2010.
Subject classification:
Seismology, Earthquake, Seismo-electromagnetism, Ionospheric perturbations, Subionospheric propagation.

ABSTRACT

The unusual variations observed in the records of the integrated field intensity of the atmospherics (IFIA) at 6 kHz and 9 kHz at Agartala, Tripura, in the north-eastern state of India (latitude, 23° N; longitude, 91.4° E) during the large earthquake on October 8, 2005 at Muzaffarabad (latitude, 34.53° N; longitude, 73.58° E) in Kashmir in Pakistan are here analyzed. Spiky variations in the IFIA at 6 kHz and 9 kHz were observed several days previous to the day of the earthquake (from midnight, September 28, 2005). The effects persisted for some days, decayed gradually, and eventually ceased on October 31, 2005. The spikes are distinctly superimposed on the ambient level, with mutual separation of 2–5 mins. The number of spikes per day and the total duration of their occurrence were particularly high on the day of the earthquake. The spike heights are higher at 6 kHz than at 9 kHz. The results are discussed here. The generation of electromagnetic radiation associated with the fracture of rocks, the subsequent penetration of this radiation into the Earth atmosphere, and finally its propagation through the Earth–ionosphere waveguide may be responsible for these observed spikes. The present observations show that the very low frequency anomaly dominates between 6 kHz and 9 kHz. The nature of the spikes presented here is a characteristic feature of the IFIA during the period of the earthquake. This has been established on the basis of time-series analyses over a period of one year.

1. Introduction

Seismic waves originate an electric field within the upper atmosphere due to the seismo-ionospheric coupling phenomena during any strong earthquake [Hayakawa 1999, Pulinets et al. 2003, Hayakawa et al. 2004]. To develop a model for earthquake forecasting, it is necessary to accumulate empirical evidence that major earthquakes are preceded by a number of minor seismic events in their neighborhood. The actual relationship between foreshocks and the subsequent large shocks of the main earthquake still need to be investigated. However, no means has been discovered by which foreshocks can be recognized in advance. Under these circumstances, it is advantageous to investigate the characteristic variations in electromagnetic noise patterns that have occurred prior to a number of large earthquakes. This requires the creation of a data bank on a global scale. Side by side, this requires a model relating to the probability of occurrence of earthquakes and the characteristic variations in the atmospheric radio noise. This is because atmospheric radio noise can be affected by seismic activity through at least two independent ways: one is the direct link between the Earth surface and the ionosphere, via acoustic waves launched from the region above the epicenter; and the other is the direct emission of radio waves prior to earthquakes. The electromagnetic precursor to an earthquake is an important issue for an understanding of the physical processes of the origin of the earthquake. Hence, to model for any earthquake, such a precursor might be an important tool for a clear understanding of the process of electromagnetic emission from a fault zone. Most studies here have concentrated on very low frequency (VLF) anomalies during earthquakes.

Many studies have reported on the emission and propagation of electromagnetic waves from large earthquakes in the extremely low frequency, ultra-low frequency, and VLF (ELF-ULF-VLF) bands [Gokhberg et al. 1982, Fujinawa and Takahashi 1998]. Satellite-based observations around earthquake zones provide both pre- and post-seismic variations in the ELF-VLF amplitudes, and also provide variations in the ionospheric parameters [Calais and Minster 1995, Molchanov and Hayakawa 1998, Pulinets 1998, Shvets et al. 2002, Liu et al. 2004]. A report on electromagnetic anomalies associated with earthquakes in Greece covered a wide range of frequencies and showed that electromagnetic anomalies correlate with the fault model characteristics of the associated earthquake and with the degree of geotectonic

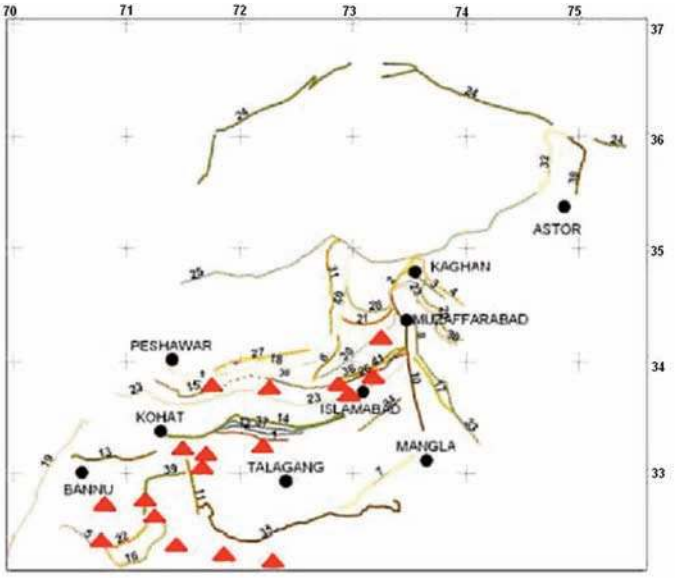

Figure 1. The positions of the various faults in the north-west Himalayas.

heterogeneity within the focal zone [Eftaxias et al. 2003].

There is no unique model that can explain electromagnetic anomalies during an earthquake. An earthquake might produce some kind of surface electric effects that might be assumed to launch electromagnetic waves. In connection with results from laboratory experiments, some studies have argued in favor of electrification due to micro-fracturing. Such accumulation of charges involves transient currents around focal areas accompanying micro-fracturing over a length of the order of that of the subsequent fracture generated by the earthquake. This is of the order of several kilometers. Considering these dimensions, the antenna theory shows that the emissions should be mainly confined to the VLF part of the electromagnetic spectrum.

In the earthquake preparation zone at the time of strong seismo-ionospheric coupling processes, underground gas discharges carry submicron aerosols with them that enhance the intensity of the electric field at the near ground due to a drop in air conductivity created by the aerosols [Krider and Roble 1986, Chmyrev et al. 1997]. Seismo-electromagnetic emissions in seismically active zones have been observed at low frequency bands prior to large earthquakes [Nagao et al. 2002]; these are different from lightning-induced and technogenic emissions. In the event of a strong earthquake, the near ground of the atmospheric layer becomes ionized and generates a strong electric field that introduces particle acceleration, thereby exciting the local plasma instabilities.

During the process of lithosphere–ionosphere coupling, the ion cluster mass and plasma concentrations vary with the size of the earthquake. As a result, the seismo-electromagnetic emissions would be expected to cover almost the whole of the ELF-ULF-VLF band. In the process, there will be increased thermal plasma noise, along with Cerenkov radiation and Bremstrallung. This sort of plasma instability at the surface can be assumed to be simulated in dusty plasma [Kikuchi 2001].

The Himalayas extend laterally for about 2,400 km, from western Kashmir to the Indo-Barman border. The ongoing convergence between the Indian and Eurasian plates has resulted in a very high level of seismicity in this region. In this area of convergence, transpressional tectonics are also found to be operative. A large number of faults have been recognized in the north-west Himalayas of Pakistan [Armbruster et al. 1978]. These include faults of very great extent, such as the Main Mantle Thrust, the Main Boundary Thrust, and the Himalayan Frontal Thrust, as well as local faults. According to a map showing the faults [MonaLisa et al. 2006, 2007], there are at least 41 active faults in the belt of the north-west Himalayas; the positions of these are indicated in Figure 1.

The Muzaffarabad-Kashmir earthquake on October 8, 2005, was the deadliest in the history of the Indian sub-continent, and it killed more than 80,000 people. This earthquake had a strength of M = 7.7 and occurred at 08:20:38, Indian Standard Time (IST) on October 8, 2005, with its epicenter at 34.53° N, 73.58° E, about 19 km north-east of Muzaffarabad and 100 km north-east of Islamabad. The depth of the epicenter of the main shock was 26 km, whereas the depths of the aftershocks were between 5 km and 20 km, among which most were at a depth of 10 km. The earthquake occurred in a rupture plane 75 km long and 35 km wide [Avouac et al. 2006, Pathier et al. 2006]. About 147 aftershocks were documented on the first day after the initial shock, one of which had a magnitude of 6.4. Twenty-eight aftershocks occurred with magnitudes greater than 5 during the four days after the main shock [MonaLisa et al. 2008]. On October 19, 2005, there was a series of strong aftershocks, one with a magnitude of M = 5.8, which occurred about 65 km north-north-west of Muzaffarabad.

The outcome of some significant observations recorded by VLF receivers at Agartala (latitude, 23° N; longitude, 91.4° E) at 1 kHz, 6 kHz and 9 kHz during this India-Pakistan border earthquake that occurred on October 8, 2005, at Kashmir (in Pakistan) are reported here. The effects of the large earthquake (M = 7.7) are manifested through the occurrence of discrete spikes. A good number of spikes were first observed on September 28, 2005, and continued up to October 13, 2005. Both the number of spikes, their intensities, and their durations were found to change in a random fashion, and they reached their maximum values on the day of occurrence of the earthquakes. The spikes then decreased gradually and almost ended after October 13, 2005. The records were taken at Agartala, which is about 2,179 km away from where the earthquake occurred. Observations were taken at Agartala continuously at frequencies of 1 Hz, 3 Hz, 6 Hz, 9 Hz and 12 kHz. None of

these effects were observed at frequencies other than 6 kHz and 9 kHz. The effects at 6 kHz were more prominent than those at 9 kHz. The data were analyzed and the outcomes of the results are presented here.

2. Instrumentation

The VLF spectra at different frequencies (1, 3, 6, 9 and 12 kHz) have been regularly recorded over the last several years from Agartala (latitude, 23° N; longitude, 91.4° E). These signals are processed and are recorded in a computer. The RMS values of the filtered data were here analyzed using Origin 5.0 software.

The receiver mainly consists of (a) an antenna (b) an AC amplifier (c) a selection circuit (d) a detection circuit (e) a logarithmic amplifier, and (f) a recording device. The receiver system is shown as a block diagram in Figure 2. The effective height of the antenna was fixed to 8.63 m, and the terminal capacitance of the antenna wire was kept at 694 pF.

An inverted L-type antenna was installed to receive vertically polarized atmospherics in the ELF-VLF bands from near and far sources. By selecting the bands using a low-pass filter, unwanted noise was reduced. The cut-off frequencies of the low-pass filter and the tuning frequencies were different. For example, to receive atmospherics at 3 kHz, the induced voltage of the antenna was passed through a low-pass filter with a cut-off frequency of 5 kHz, as shown in Table 1. The filter output was amplified with an AC amplifier using an OP AMP IC531 in a non-inverting mode. The gain was limited within the value to check transients that might trigger sustained oscillations in the amplifier. The amplifier was followed by a series resonant circuit that was tuned to the desired frequency, and another buffer.

To have good selectivity (low bandwidth), the induction coil was mounted inside a pot-core of ferrite material. The selected sinusoidal Fourier components of the atmospherics were then passed to the input of a detector circuit through a unit gain buffer, using the OP AMP IC531. In the detector circuit, the OA79 diode was used in the negative rectifying mode. The output of the diode was across a parallel combination of resistance and capacitance. The level of the detected envelope was proportional to the RMS of the Fourier component.

The RMS output after detection was amplified by a quasi-logarithmic DC amplifier, using the OP AMP 741 in the DC mode of operation. The recording time constant of the RMS was 15 s. The calibration of the recording system was achieved using a standard signal generator with an accuracy of ±0.86 dB. During the calibration, the antenna was disconnected from the filter circuit and replaced by the signal generator through a capacitance equal to the terminal capacitance of the antenna. At first, the outputs were calibrated in terms of the RMS of induced voltages at the antenna. To obtain very low signals from the function generator, a dB-attenuator was used. The output was calibrated in terms of the values of dB above 1 μV. Then this was converted to an absolute RMS, in units of μV. The absolute value of the induced voltage was divided by the effective height of the antenna to calculate the field strength, in μV/m.

The RMS of IFIA were recorded by a digital technique, using a data acquisition system. The digital data acquisition system used a PCI 1050, 16-channel 12-bit DAS card (Dynalog). This has a 12-bit A/D converter, 16 digital inputs and 16 digital outputs. The input multiplexer has a built-in over-voltage protection arrangement. All of the I/O parts were accessed by the 32-bit I/O instructor, thereby increasing the data input rate. This was supported by a powerful 32-bit API, which functioned for the I/O processing under the Win 98/2000 operating system. The RMS voltage detected was sampled at the rate of 1 Hz.

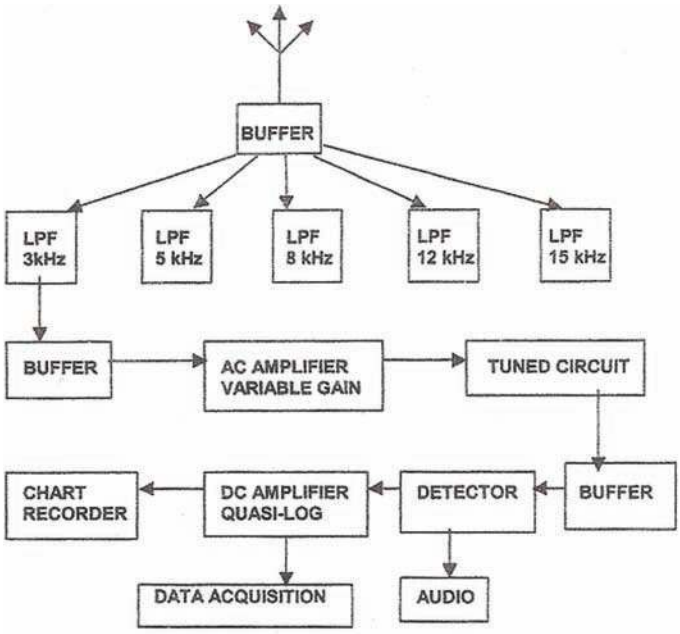

Figure 2. Diagram of the ELF-VLF receiving system at Agartala (latitude, 23° N; longitude, 91.4° E).

Cut-off frequency (low-pass filter) (kHz)	Tuned frequency (kHz)
3	0.900 (in lieu of 1)
5	3
8	6
12	9
15	12

Table 1. Cut-off frequency of low-pass filter, and corresponding tuned frequencies.

3. Observations

The IFIA in the VLF band at frequencies of 1 kHz, 3 kHz, 6 kHz, 9 kHz and 12 kHz showed various features. These were recorded simultaneously at Agartala (latitude, 23° N; longitude, 91.4° E), around-the-clock. The monsoon record is very different from the winter records. The differences between the daily maximum and daily minimum can be of the order of 12-16 dB during the monsoon, whereas it is 8-13 dB in winter. Figure 3 shows the time series data of IFIA at 1 kHz, 6 kHz and 9 kHz for the one-year period from February 2005 to January 2006, except for the days of the earthquake periods. Figure 4 shows the records

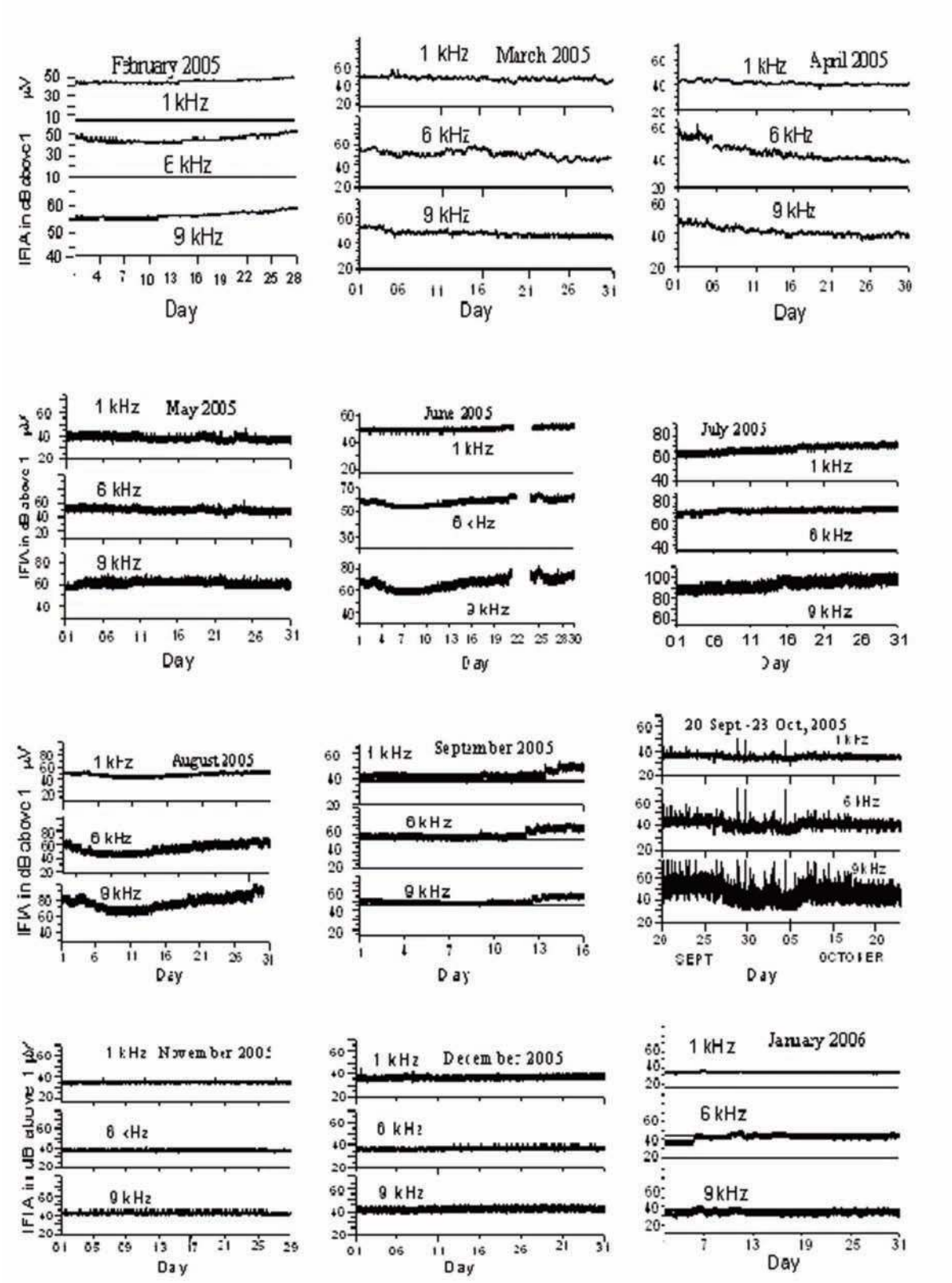

Figure 3. Time series records of the IFIA at 1 kHz, 6 kHz and 9 kHz for the months of February 2005 to January 2006.

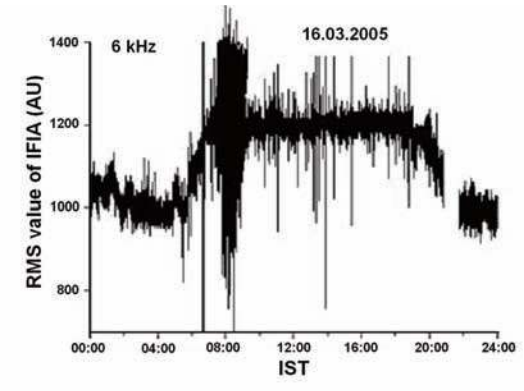

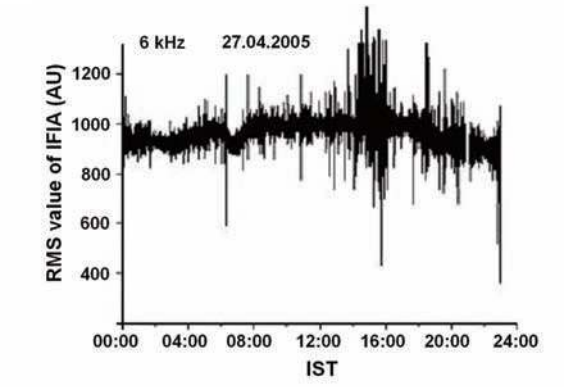

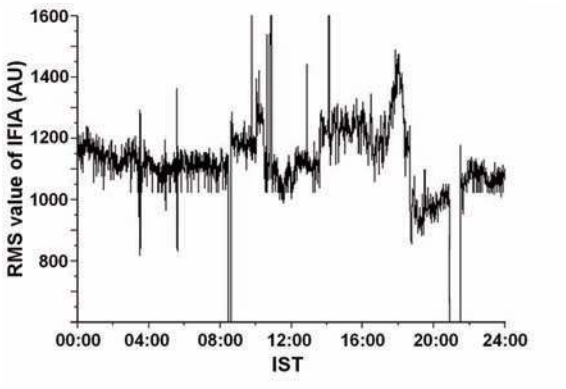

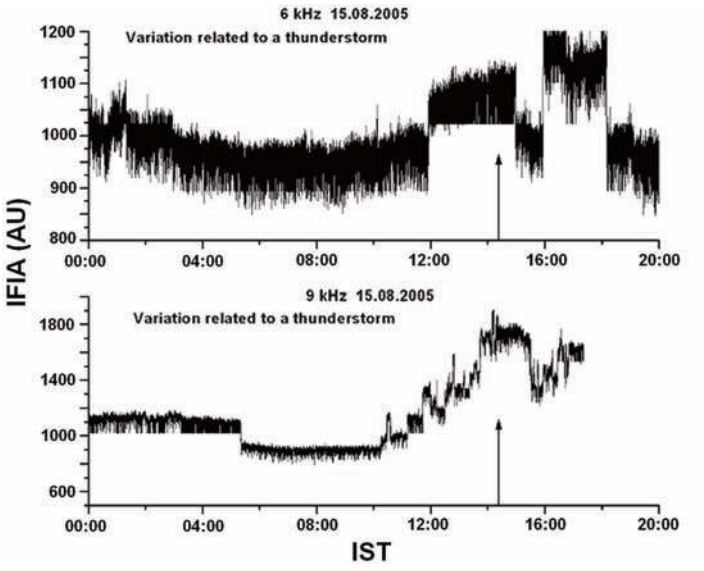

during an overhead shower that occurred from 07:10 to 09:15 hours IST on March 16, 2005. The record shows large numbers of transient variations during the period of the shower. Figure 5 shows the record of the IFIA on April 27, 2005. Rain occurred within a radius of 10–15 km, and partially overhead rain occurred along with lightning from 14:15 to 16:05 hours IST. Again large numbers of transient variations are observed. The transient levels were more than 50% both above and below the ambient level during the overhead shower with thunder and lightning activity within a radius of 10–15 km. Figure 6 shows the records of the IFIA on a day in which a thunderstorm occurred in south Tripura, at a distance of about 40–50 km from the receiving station. Although small in number, transient variations were found. A typical record of the IFIA at 6 kHz and 9 kHz during a thunderstorm at north Tripura at a distance of 75–100 km is shown in Figure 7, where the arrow mark indicates the onset of the rain. Figure 8 shows that during a distant thunderstorm that occurred at about midday, the IFIA was enhanced gradually, and then decreased very sharply. In the case of distant cloud activity, the level of the IFIA increased. We explored data over one year and found that any kind of distant lightning activity only changes the level of the IFIA, and does not produce any transient variations in the IFIA levels.

Remarkable spiky variations in the records at 6 kHz and 9 kHz were observed some days prior to the vast earthquake at Muzaffarabad (latitude, 34.53° N; longitude, 73.58° E) on October 8, 2005. Spikes of appreciable intensity appeared first at midnight on September 28, 2005 (Figure 9). Large spikes also appeared prominently on October 5, 2005, only in the records of the 6 kHz and 9 kHz frequencies, which are shown in Figure 10. The number of dominant spikes and their durations increased until they reached their maximum values on the day of the main earthquake. In the time scale, the spikes had a duration of about a few minutes. If the

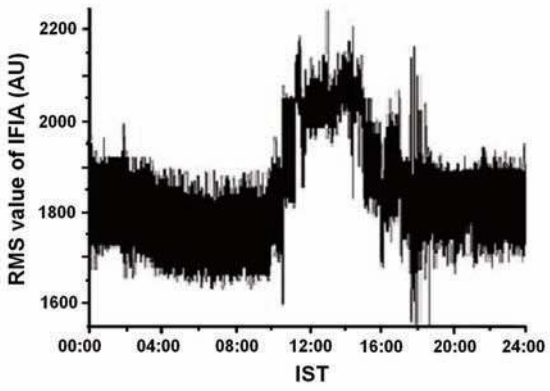

From up to bottom, left to right: **Figure 4.** Record of the IFIA on a rainy day with an overhead shower from 07:10 to 09:15 hours IST. **Figure 5.** Record of the IFIA on a rainy day with an overhead shower from 14:15 to 16:05 hours IST. **Figure 6.** Record of the IFIA in relation to thunderstorm activity in south Tripura at distance of 40–50 km from the receiving station. **Figure 7.** Typical record of the IFIA at 6 kHz and 9 kHz during a thunderstorm over north Tripura at a distance 75–100 km from the receiving station. Arrow, onset of the rain associated with the thunderstorm. **Figure 8.** Typical record of the IFIA at 6 kHz during a thunderstorm over North Tripura at a distance 75–100 km from the receiving station.

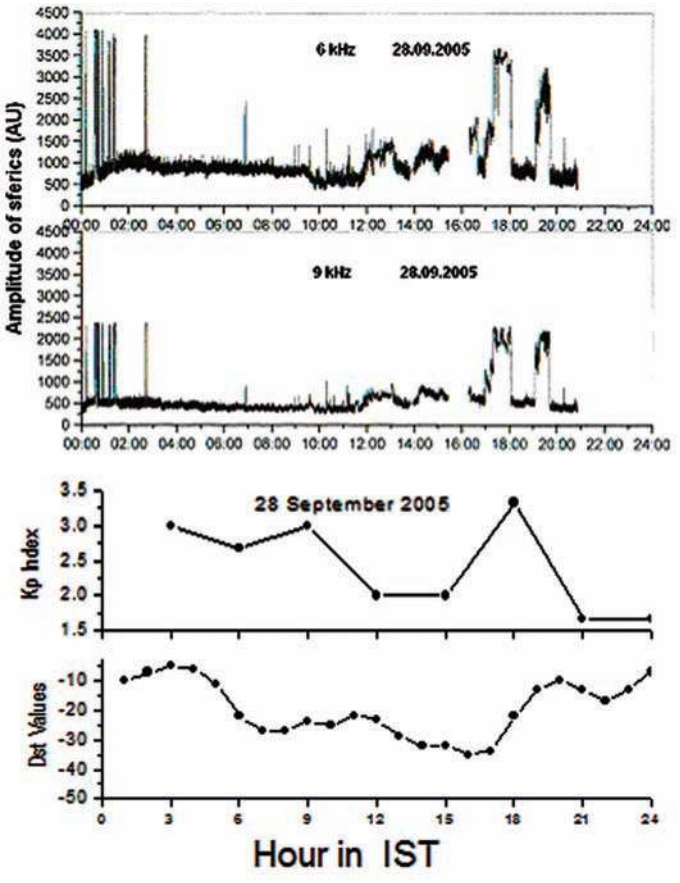

Figure 9. Diurnal variations of the IFIA at 6 kHz and 9 kHz, and of the Kp index and Dst, for Agartala on September 28, 2005.

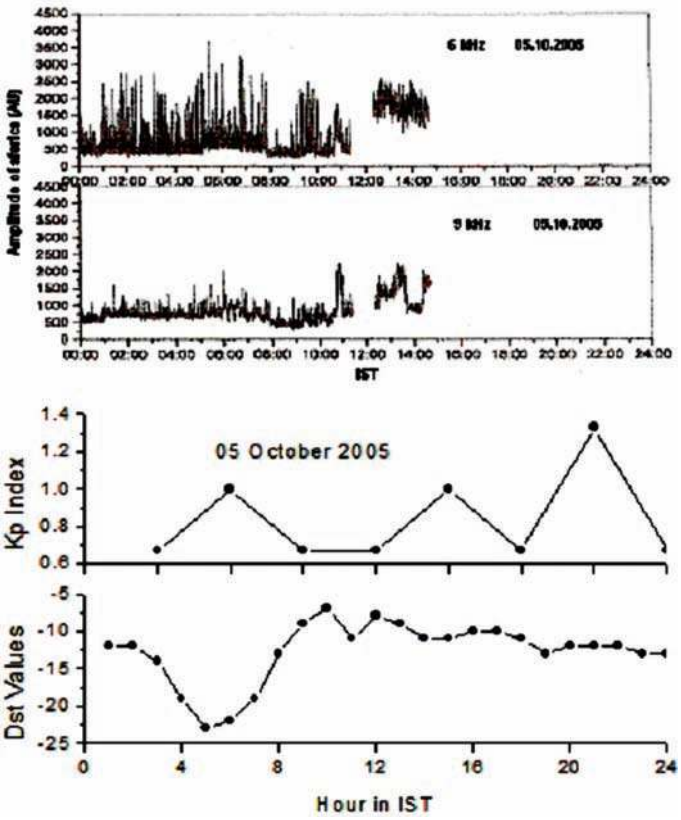

Figure 10. Diurnal variations of the IFIA at 6 kHz and 9 kHz, and of the Kp index and Dst, for Agartala on October 5, 2005. The IFIA data from 15:00 to 24:00 IST are missing.

recorded data of 24 h is shown on A4-size paper, the sudden large variations in IFIA with durations of a few minutes would appear as spikes. The nature of these spikes is completely different from the transient variations that occurred due to local or distant thunderstorms. The rate of sampling of 1 Hz of the DC level was sufficient to detect variations in duration of a few minutes. The spike heights are high compared to those of the ambient spikes of transient variations in atmospheric sources. This means that although the absolute values of the IFIA were low during September and October, even here the enhancement above the ambient level was higher during the earthquake, as compared to during the atmospheric activity.

It was initially doubtful whether the appearance of these spikes represented the signatures of geophysical phenomena or local noise. The first point is that the experimental site was selected to keep the receivers away from man-made noise. The experimental site is in a rural place, at 10–12 km from the nearest town, so there was no question of man-made noise. The electric wiring in the building concerned was thoroughly checked to reveal any fault that might have produced discharges that would give spikes in the record; no such fault was present. The spikes were in some cases present during the post-midnight period, when there should not be any possibility of man-made noise, as the locality is purely a rural place that is free from both small and large industries. It is worth mentioning that occasionally a few isolated spikes were present in the records, and these were due to the operation of electrical equipment. The nature of the spikes associated with the earthquake and their characteristic separation are completely different from various known effects, e.g., solar flare effects, meteor shower effects, or geomagnetic storms. During solar flares, the atmospherics show a sudden enhancement and a gradual fall, which lasts for a time interval that is equal to or slightly longer than the duration of the flare [Thomson and Clilverd 2001, McRae and Thomson 2004, De et al. 2009]. During a meteor shower, the atmospherics show a sudden rise followed by a sudden fall, with a duration from several minutes to half an hour or so [Sarkar and De 1985, De et al. 2006]. During geomagnetic storms, the night-time levels show quasi-periodic variations of periodicity of from half an hour to several hours [Sarkar and De 1991]. So we can say that these spikes recorded are typically correlated with earthquakes.

Between September 15, 2005, and October 31, 2005, there were no meteorological phenomena, such as thunderstorms or cyclones, or heavy showers on the path between Muzaffarabad (latitude, 34.53° N; longitude, 73.58° E) and Agartala (latitude, 23° N; longiude, 91.4° E). There were only some scattered thundershowers after 22:00 hours IST on October 8, 2005, until midnight, and to 02:00 hours IST. This has been confirmed by the weather report from

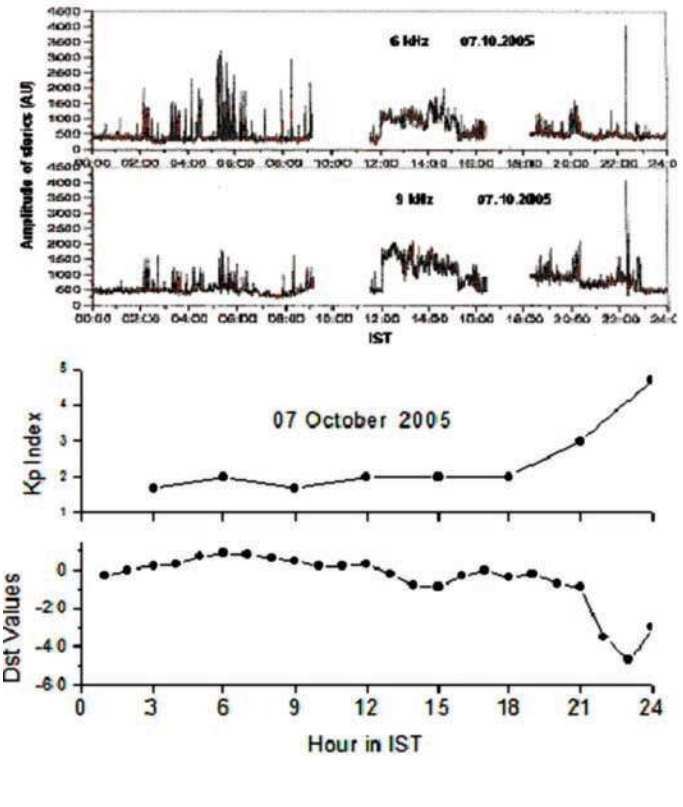

Figure 11. Diurnal variations of the IFIA at 6 kHz and 9 kHz, and of the Kp index and Dst, for Agartala on October 7, 2005.

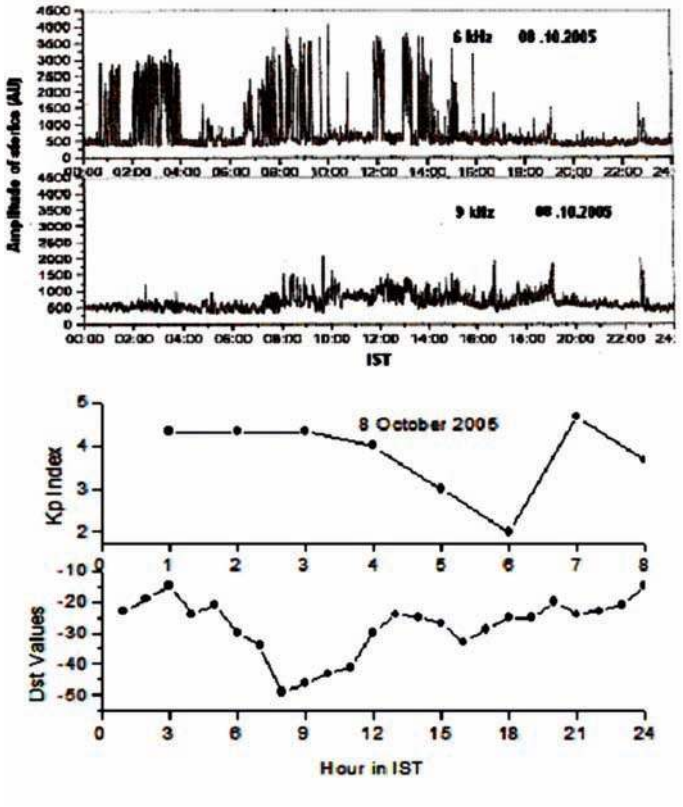

Figure 12. Diurnal variations of the IFIA at 6 kHz and 9 kHz, and of the Kp index and Dst, for Agartala on October 8, 2005, the day of the earthquake.

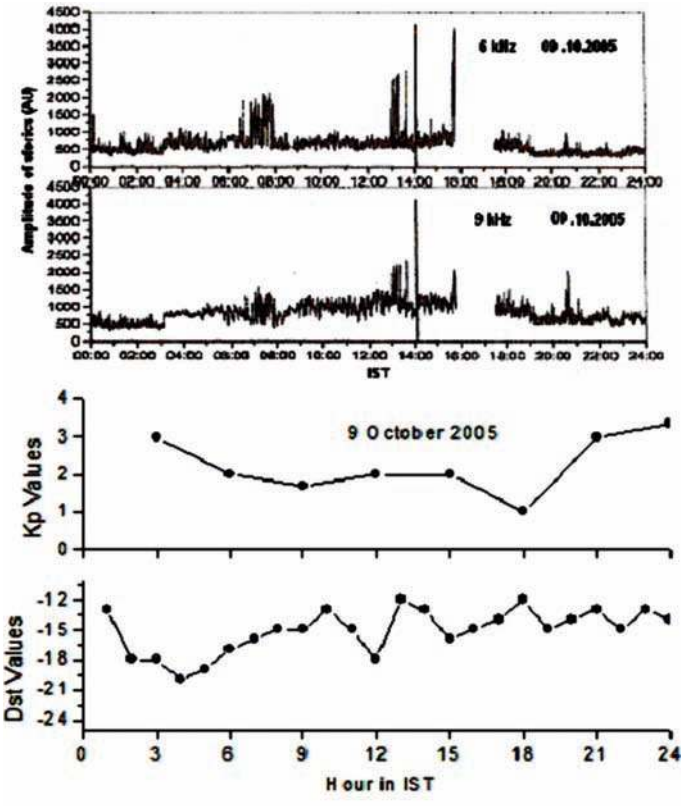

Figure 13. Diurnal variations of the IFIA at 6 kHz and 9 kHz, and of the Kp index and Dst, for Agartala on October 9, 2005.

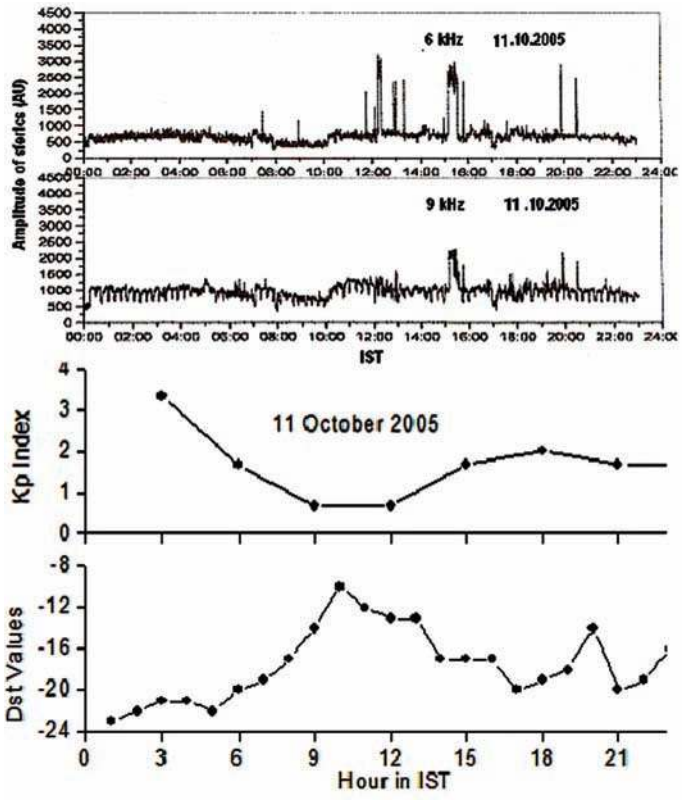

Figure 14. Diurnal variations of the IFIA at 6 kHz and 9 kHz, and of the Kp index and Dst, for Agartala on October 11, 2005.

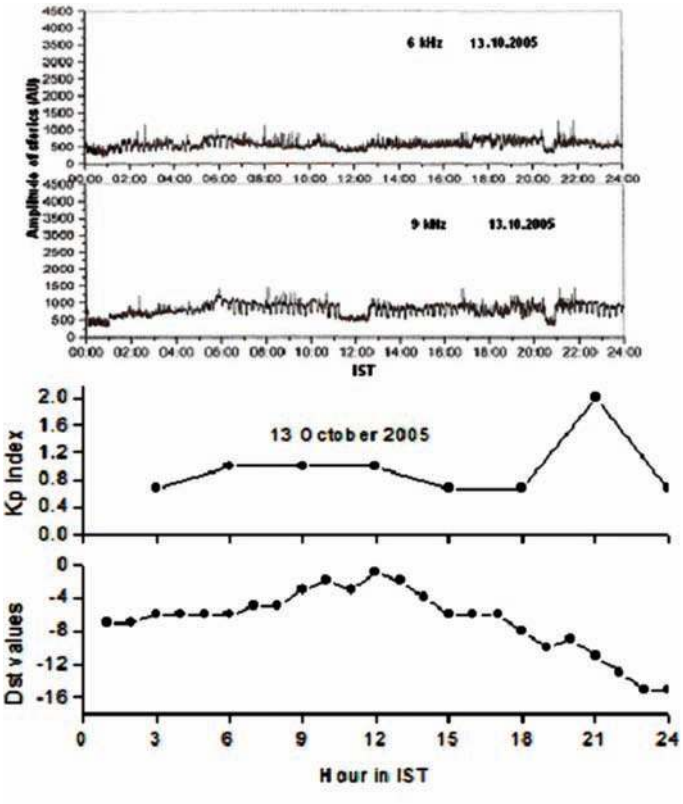

Figure 15. Diurnal variations of the IFIA at 6 kHz and 9 kHz, and of the Kp index and Dst, for Agartala on October 13, 2005.

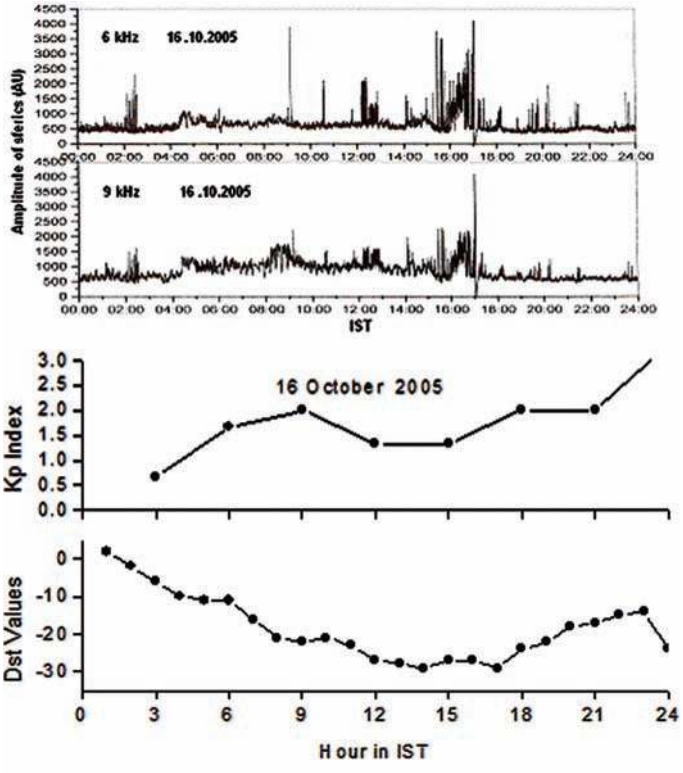

Figure 16. Diurnal variations of the IFIA at 6 kHz and 9 kHz, and of the Kp index and Dst, for Agartala on October 16, 2005.

the website http://www.imd.gov.in/city_weather/station/agartala.htm. The difference in IFIA during the thunderstorms and the spikes in the IFIA during the earthquake can be seen by the comparison of Figures 4 to 8 with Figures from 9 to 16. Figures 4 to 8 show the variations in the IFIA at 6 kHz and 9 kHz that are due to thunderstorm activity, and Figures 9 to 16 show the spiky variations that are associated with the earthquake. The diurnal variation of Dst and Kp over the corresponding dates are also plotted in Figures 9 to 16, to check whether there was any severe magnetic activity on these dates or not. In the case of the earthquake-related events, the spikes maintain an interval of the order of 2–5 min on average. The transient variations in IFIA produced by thunderstorms consist of remarkable changes in the base level, and these kinds of changes also extended downwards. The spikes related to earthquakes are distinct from each other and the base level remains almost constant, without being extended downwards.

During the day of the earthquake, the number of spikes above the ambient level was very high and the intensity (height) of the spikes above the ambient value was also remarkably high. The spikes commenced a few days prior to the day of the earthquake, so these might represent precursors of the earthquake. The intensity of the spikes gradually reduced, and then almost ceased after October 31, 2005. The effects at 6 kHz were greater than at 9 kHz.

Some typical features of the records during the period between September 15, 2005, and October 31, 2005, are presented in Figures 9 to 16. We now define the normalized value of the number of spikes in a day as:

$$\text{Normalized value} = \frac{\text{Number of spikes observed in a day} \times 24 \text{ hours}}{\text{Period of observation in a day}}$$

Figure 17 shows the day-to-day variation in the number of spikes (as normalized values) for the period from September 15, 2005, to October 31, 2005. The intensity of the spikes in arbitrary units (AU) on different days before and after the earthquake are shown in the histogram in Figure 18. It can be seen that on the day of the main shock, the response at 6 kHz was much higher than at 9 kHz. Both the pre- and post-earthquake effects were different at these two frequencies.

The receiver gain is different during different seasons. During the monsoon month, the receiver gain was kept low due to the higher level of atmospherics, both in amplitude and in the rate of their occurrence. So the IFIA was high. During this period, as the gain was kept low, the large increase in the level appears to be smaller. During the months from the end of September to February, the receiver gain was higher due to the low IFIA. So there is an apparent anomaly regarding the magnitude of enhancement that arises when the variations due to the thunderstorm and due to the earthquake are compared directly.

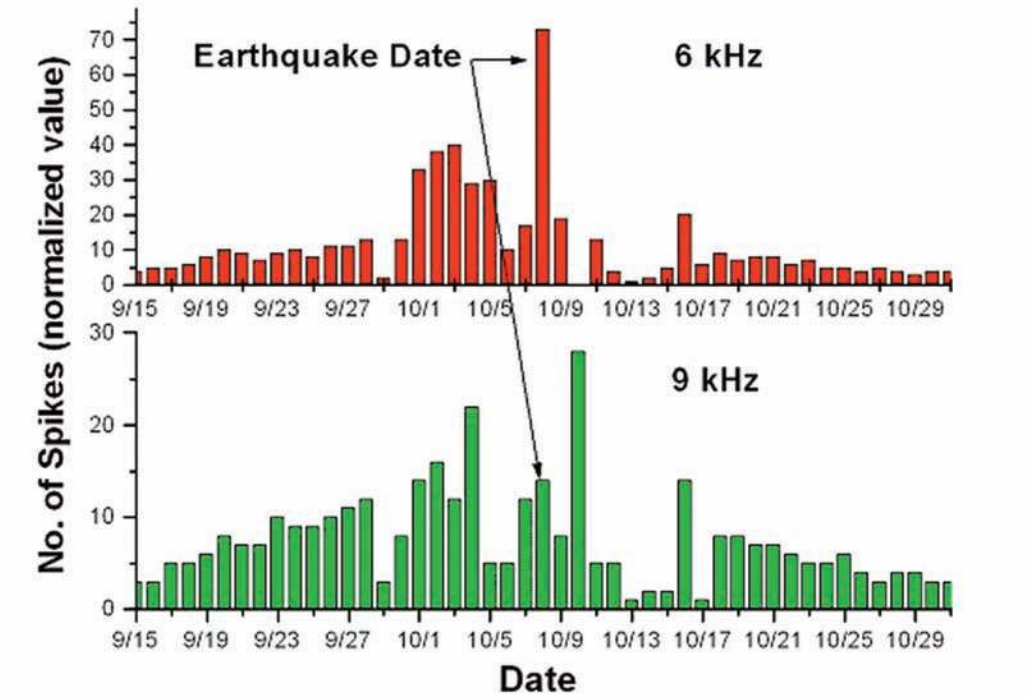

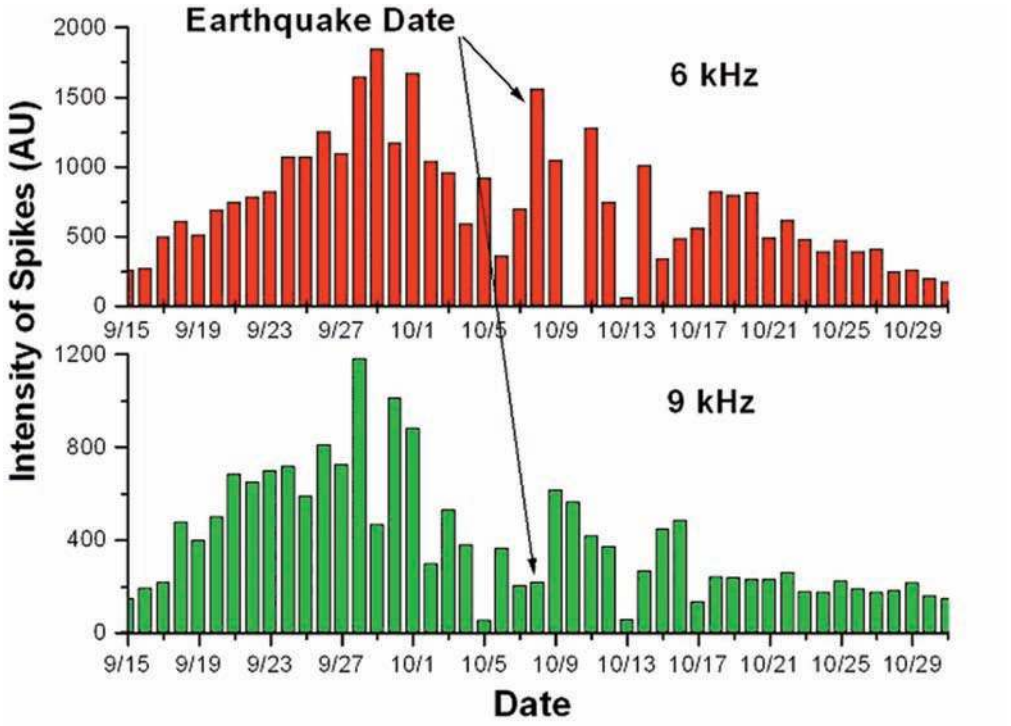

Figure 17 (up). Variations of the number of spikes (normalized value) at 6 kHz and 9 kHz before and after the earthquake.
Figure 18 (bottom). Variations of the intensity of the spikes at 6 kHz and 9 kHz above the ambient level before and after the earthquake.

It is worth mentioning that a new project has now been started, through which the IFIA will be studied at various places in the north-eastern parts of India, including the northern regions of west Bengal and Sikkim. For this purpose, we have selected Mirik (latitude, 26.9° N; longitude, 88.17° E) to collect data of the IFIA at 3 kHz and 9 kHz. Mirik is a hill station in India, which was built around a 1.25-km-long natural lake at an altitude of 1,767 m a.s.l. In a campaign mode, we have collected the IFIA data during the various seasons. The 9 kHz IFIA data recorded during some specific times of the day at Mirik showed spiky variations from October 2, 2005, to October 7, 2005. In Figure 19, these spiky variations in the IFIA as observed in the Mirik data are presented. The Mirik data were only for one week and also for small periods for each day of the campaign. These observations support the spikes observed in the records of the IFIA at Agartala.

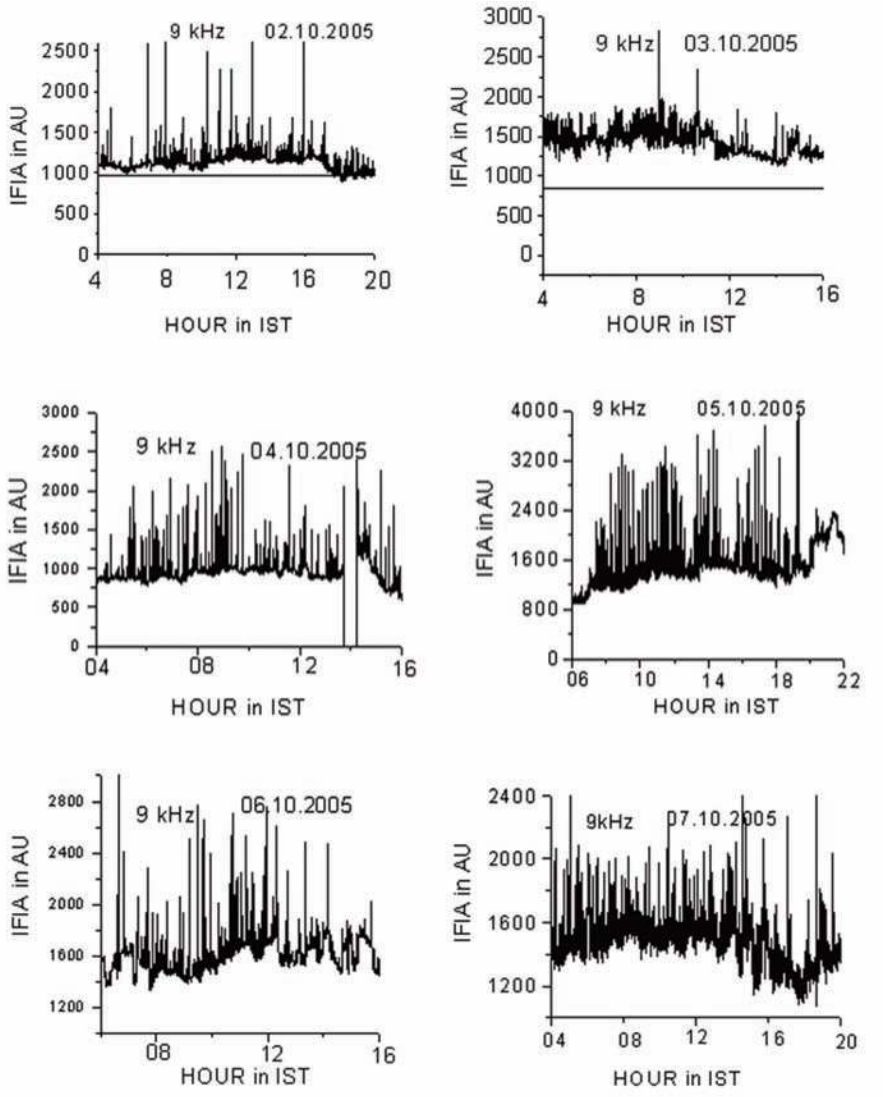

Figure 19. Variations of the IFIA at 9 kHz recorded from October 2–7, 2005, at Mirik (latitude, 26.9° N; longitude, 88.17° E).

4. Discussion

Although the ionospheric perturbations as detected by VLF-LF propagation are now considered to be a significant tool for short-term earthquake prediction, it has also been reported that several days before the occurrence of an earthquake, the electron density of the plasma in the upper ionosphere over the epicenter also shows extraordinary changes. Moreover, there are interrelations between the tectonic activity and the anomalous changes in the geophysical, geochemical and geohydrological parameters that characterize the Earth lithosphere. As a result, there will be thermal plasma instability; seismo-electromagnetic emissions would be expected to cover almost the whole of the ELF-ULF-VLF band.

To ascertain that the magnetic activity does not have any significant role, we have plotted the diurnal variation of Dst and Kp in Figures 9 to 16, *vis-à-vis* the records of the atmospherics. The planetary or Kp index ranges between 0 and 9. The values of this index give a good indication of the geomagnetic activity, whereby values between 0 and 1 indicate quiet magnetic conditions. The values of Kp indicating the magnetic status are shown in Table 2.

The Dst index is a measure of the variations in the geomagnetic field due to the equatorial ring current. At a given time, the Dst index is the average of the variations of the H-component over all longitudes. The reference level is selected such that Dst is statistically zero on internationally designated quiet days. An index smaller than −50 nT indicates the absence of magnetic disturbance. The plots of Dst and Kp show that the period of observation of the spikes was devoid of magnetic disturbance.

An anomalous increase in the electromagnetic radiation at 27 kHz, 385 kHz and 1.63 MHz before a large main shock (M = 7.4) of an Iranian earthquake were observed in a tunnel 50 m below the ground in Caucasus, by Gokhberg et al. [1979]. Gokhberg et al. [1982] also observed similar increases in the electromagnetic radiation at 81 kHz before some earthquakes. In laboratory experiments, electromagnetic radiation associated with fractures of rock has been detected [Ogawa et al. 1985]. The occurrence of anomalous

electromagnetic noise at 163 kHz for a few hours to several days before and after the main shocks of shallow earthquakes in island areas or in shallow sea regions have been reported [Oike and Ogawa 1982]. Impulsive electromagnetic noise bursts of seismogenic emissions at 82 kHz and 1.525 kHz have been detected prior to earthquakes [Gokhberg et al. 1982, Takeo et al. 1992]. All of these observations and analyses of seismogenic emissions are found to be related to large rock crushes [Yoshino and Tomizawa 1989]. The penetration characteristics of the electromagnetic emissions from an underground seismic source into the atmosphere, ionosphere and magnetosphere have been thoroughly discussed [Molchanov et al. 1995]. A report of pulse-like electromagnetic signals associated with earthquakes in the frequency range of 1–10 kHz was given by Asada et al. [2001]. The association of the VLF emissions with the occurrence of earthquakes has been inferred from the matched temporal correlation between the direction of the VLF signal arrival and that of the epicenter. In four cases, the maximum of the VLF activity was seen 1–4 days before the earthquakes. As the time of the maximum VLF emission does not coincide with the time of the maximum shock, the earthquake must be considered to constitute an important element in the VLF emission mechanism.

Underground water diffusion in a region associated with deformation of the Earth crust prior to any earthquake raises the electrical conductivity in the crust [Ishido and Mizutani 1981]. Thus, to explain the electromagnetic radiation associated with earthquakes and volcanic activity, there is the need to calculate the attenuation of the ELF/VLF waves in the dry crust and in wet soil.

Now, the electric field of the electromagnetic waves can be expressed as [Ondoh 1992]:

$$\vec{E} = \vec{E}_0 \exp\{j(\omega t + \vec{k}.\vec{r})\} \tag{1}$$

where $\vec{k}$ is the wave vector given by $k^2 = \varepsilon\mu\omega^2 - j\sigma\mu\omega$, where ω is the angular wave frequency, $\vec{r}$ the radial vector from the radiation source, μ the permeability, ε the dielectric constant, and σ is the electrical conductivity. The complex wave number is given by $k = \alpha + j\beta$, $(\alpha > 0, \beta \cong 0)$, α represents the propagation constant and β is the attenuation constant. The attenuation constant is derived as [Ondoh 1992]:

$$\begin{aligned} \beta &= \omega\left\{ \varepsilon\mu \Big/ 2\left(\sqrt{1 + (\sigma/\varepsilon\omega)^2}\right) - 1 \right\}^{1/2} \\ &= (\sigma\mu\omega/2)^{1/2} = 1/\delta \text{ for } \sigma/\varepsilon\omega >> 1, \end{aligned} \tag{2}$$

where δ is the skin depth. The dielectric constant is expressed by $\varepsilon = \varepsilon_0\varepsilon_r$, where $\varepsilon_0 = 1/(36\pi \times 10^9)\, F/m$ is the dielectric constant or permittivity of free space, and ε_r is the relative dielectric constant. The magnetic permeability μ is usually approximated by the permeability of a vacuum $\mu_0 = 4\pi \times 10^{-7}\, H/m$, if the material concerned is not ferromagnetic. The relative dielectric constants ε_r of the material concerned are as follows: 1 for gas, 80 for water at 20 °C, and 55 for water at 100 °C. The electric conductivities σ of the material concerned are as follows: 10^{-2} mho/m for wet soil, and 10^{-5} mho/m for dry crust. The expression of $\beta = 1/\delta$ can be correctly used for electromagnetic wave attenuation below 100 kHz in wet soil and below 10 kHz in dry crust. For frequencies from 100 Hz to 10 kHz, the attenuation of the electromagnetic waves in the dry crust is less than 4 dB/km, while in wet soil, it is from 17.3 dB/km at 100 Hz and above 100 dB/km at 1 kHz. Therefore, if the electromagnetic field is generated in the dry crust by rock fractures over a vast region before and after the main shock of a shallow earthquake, anomalous electromagnetic waves will be observed even in the VLF band. During earthquakes, this spiky type of VLF excitation in the presence of an anomalous electric field has also been reported and assessed [Bardakov et al. 2004].

Kp Index	Description
0	Quiet
1	Quiet
2	Unsettled
3	Unsettled
4	Active
5	Minor storm
6	Major storm
7	Severe storm
8	Very major storm

Table 2. Relationship between Kp and magnetic storms.

The present observations are only confined to 6 kHz and 9 kHz. The poor presence of spikes below 6 kHz might be due to the attenuation of signals in the Earth–ionosphere waveguide during their propagation.

It is worth mentioning that based on a study of pre-seismic electromagnetic signals, Kapiris et al. [2002] attempted to establish a set of necessary conditions with reference to the underlying critical stage of the earthquake-generation process. Moreover, Eftaxias et al. [2002] evaluated the electromagnetic signals in terms of their relationships with earthquakes, in comparison with laboratory measurements on rock samples.

5. Conclusions

In the analysis of any earthquake activities, the magnitude and depth are known. During this India–Pakistan border earthquake, the majority of the 251 aftershocks were in the range M = 4.0–5.9. Two of them had M > 6. All of these earthquakes are not connected with the same active

faults from which the seismic activities are generated from their corresponding distinct levels. Based on shock distribution, a wide area of length of about 200 km, with a breadth of about 50 km, are found to be activated. The ruptured area is estimated to be about 1,500 square km, as determined through slip distribution [Singh et al. 2006, MonaLisa et al. 2008]. Nearly 147 aftershocks occurred on the first day after the main shock on October 8, 2005. Among these, 28 shocks occurred with magnitudes $M > 5$ during the four days after the main shock. A series of moderately strong aftershocks were documented on October 19, 2005, one of which had a magnitude $M > 5.8$. The occurrences of aftershocks then gradually decayed with time, and finally almost ceased towards the end of April, 2006. The distribution of the depths of the aftershocks was in the range of 5–20 km. Thus, the effects of the seismological activity of the main earthquake on October 8, 2005, and the subsequent aftershocks of different magnitudes and depths were perceived randomly at the surface. Due to this, the heights and numbers of pre- and post-earthquake spikes in Figures 17 and 18 are not systematically distributed around the spikes during the main shock, and the heights of bars in the statistical analysis are highly irregular.

The strength of the electromagnetic component at the receiving station is controlled by the source strength, the attenuation in the Earth crust from the source to the surface, and the attenuation in the Earth–ionosphere waveguide. The effect is good at a frequency of around 6 kHz, although the propagation in the Earth–ionosphere waveguide is good at 9 kHz. This implies that the intensity of the spectral component of the electromagnetic pulse associated with an earthquake is much higher at 6 kHz than at 9 kHz. At the same time, it should be noted that the electromagnetic wave at 9 kHz is attenuated within the Earth crust to a greater extent than at 6 kHz, while traveling from the source region to the surface of the Earth. This spectral behavior might represent a tool to identify whether an electromagnetic pulse is due to an earthquake or due to other reasons. The present study also demonstrates that an electromagnetic pulse due to an earthquake might not be detectable at all VLF frequencies at a receiving station.

Acknowledgments. This study is funded by the Indian Space Research Organization (ISRO) through the S. K. Mitra Centre for Research in the Space Environment, University of Calcutta, Kolkata, India. The authors are thankful to the reviewers of the manuscript for the critical comments and constructive suggestions, which were incorporated into this revised version.

References

Armbruster, J., G.L. Seeber and K.K. Jacob (1978). The northwest termination of the Himalayan mountain front: active tectonics from micro earthquakes, J. Geophys. Res., *83*, 269-282.

Asada, T, H. Baba, M. Kawazoe and M. Sugiura (2001). An attempt to delineate very low frequency electromagnetic signals associated with earthquakes, Earth Planets Space, *53*, 55-62.

Avouac, J.P., F. Ayoub, S. Leprince, K. Konca and D.V. Helmberger (2006). The 2005 Mw 7.6 Kashmir earthquake: sub-pixel correlation of ASTER images and seismic wave from analysis, Earth Planet Sci. Lett., *249*, 514-528.

Bardakov, V.M., B.O. Vugmeister, A.V. Petrov and A. Chramtsov (2004). Excitation of VLF-signals under earthquake preparation process, Annual Report of Irkutsk State Technical University, Irkutsk., 16 pp.

Calais, E. and J.B. Minster (1995). GPS detection of ionospheric TEC perturbations following the January 17, 1994, Northridge earthquake, Geophys. Res. Lett., *22*, 1045-1048.

Chmyrev, V.M., N.V. Isaev, O.N. Serebryakova, V.M. Sorokin and Y.P. Sobolev (1997). Small-scale plasma inhomogeneities and correlated ELF emissions in the ionosphere over an earthquake region, J. Atmos. Sol.-Terr. Phys., *59*, 967-974; doi: 10.1016/S1364-6826(96)00110-1.

De, B.K., S.S. De, B. Bandyopadhyay, S. Paul, S. Barui and D.K. Haldar (2009). Some studies on solar flare effects on the propagation of sferics and a transmitted signal, Indian J. Radio Space Phys., *38*, 260-265.

De, S.S., B.K. De, A. Guha and P.K. Mandal (2006). Detection of 2004 Leonid meteor shower by observing its effect on VLF transmission, Indian J. Radio Space Phys., *35*, 396-400.

Eftaxias, K., P. Kapiris, E. Dologlou, J. Kopanas, N. Bogris, G. Antonopoulos, A. Polygiannakis, A. Peratzakis and V. Hadjicontis (2002). EM anomalies before the Kozani earthquake: a study of their behaviour through laboratory experiments, Geophys. Res. Lett., *29*, 1228; doi: 10.1029/2001GL013786.

Eftaxias, K., P. Kapiris, A. Polygiannakis, A. Peratzakis, J. Kopanas, G. Antonopoulos and D. Rigas (2003). Experience of short-term earthquake precursor with VLF-VHF electromagnetic emissions, Nat. Hazard. Earth Sys., *3*, 217-228.

Fujinawa, Y. and K. Takahashi (1998). Electromagnetic radiations associated with major earthquakes, Phys. Earth Planet. In., *105*, 249-259.

Gokhberg, M.B., V.A. Morgounov and E.L. Aronov (1979). On high frequency electromagnetic radiation during seismic activity, Dokl. Akad. Nauk., *248*, 1077-1087.

Gokhberg, M.B., V.A. Morgounov, T. Yoshino and L. Tomizawa (1982). Experimental measurement of electromagnetic emissions possibly related to earthquake in Japan, J. Geophys. Res., *87*, 7824-7827.

Hayakawa, M. (1999). Atmospheric and Ionospheric Electromagnetic Phenomena Associated with Earthquakes, Terra Sci. Pub. Co., Tokyo.

Hayakawa, M., O.A. Molchanov and NASDA/UEC team (2004). Achievements of NASDA's earthquake remote sensing frontier project, Terr. Atmos. Oceanic Sci., *15*, 311-327.

Ishido, T. and H. Mizutani (1981). Experimental and theoret-

ical basis of electrokinetic phenomena in rock-water systems and its applications to geophysics, J. Geophys. Res., 86, 1763-1775.

Kapiris, J., J.P. Polygiannakis, A. Peratzakis, K. Nomikos and K. Eftaxias (2002). VHF-electromagnetic evidence of the underlying pre-seismic critical stage, Earth Planets Space, 54, 1237-1246.

Kikuchi, H. (2001). Electrodynamics in dusty and dirty plasmas, Kluwer Academic Publishers.

Krider, E.P. and R.W. Roble, eds. (1986). The Earth's Electrical Environment, National Academy Press, Washington D.C.

Liu, J.Y., Y.J. Chuo, S.J. Shan, Y.B. Tsai, S.A. Pulinets and S.B. Yu (2004). Pre-earthquake ionospheric anomalies monitored by GPS TEC, Ann. Geophys., 22, 1585-1593.

McRae, W.M. and N.R. Thomson (2004). Solar flare induced ionospheric D-region enhancements from VLF phase and amplitude observations, J. Atmos. Sol.- Terr. Phys., 66, 77-87; doi: 10.1016/j.jastp.2003.09.009.

Molchanov, O.A. and M. Hayakawa (1998). Subionospheric VLF signal perturbations possibly related to earthquakes, J. Geophys. Res., 103, 17,489-17,504.

Molchanov, O.A., M. Hayakawa and V.A. Rafalsky (1995). Penetration characteristics of electromagnetic emissions from an underground seismic source into the atmosphere, ionosphere, and magnetosphere, J. Geophys. Res., 100, 1691-1712.

MonaLisa, A.B. Kausar, A.A. Khwaja and M.Q. Jan (2006). 8 October 2005 Pakistan earthquake: preliminary observations and report of an international conference at Islamabad, Pakistan, 18–19 January, 2006, Episodes, 20, 5-7.

MonaLisa, A.A. Khwaja and M.Q. Jan (2007). Seismic hazard assessment of the NW Himalayan fold-and-thrust belt, Pakistan, using probabilistic approach, J. Earthquake Eng., 11, 257-301.

MonaLisa, A.A. Khwaja and M.Q. Jan (2008). The 8 October 2005 Muzaffarabad earthquake: preliminary seismological investigations and probabilistic estimation of peak ground accelerations, Current Science, 94, 1158-1166.

Nagao, T., Y. Enomoto, Y. Fujinawa, M. Hata, M. Hayakawa, I. Huang, Q. Izutsu, Y. Kushida, K. Maeda, K. Oike, S. Uyeda and T. Yoshino (2002). Electromagnetic anomalies associated with 1995 KOBE earthquake, J. Geodynamics, 33, 401-411.

Ogawa, T., K. Oike and T. Miura (1985). Electromagnetic radiations from rocks, J. Geophys. Res., 90, 6245-6249.

Oike, K. and T. Ogawa (1982). Observations of electromagnetic radiation related with the occurrence of earthquakes, Ann. Rep., Disaster Prevention Res. Inst., Kyoto Univ., 25, 89-100.

Ondoh, T (1992). Observations on LF atmospherics associated with lightning discharges in volcano eruption smoke, Res. Lett. Atmos. Electr., 12, 235-251.

Pathier, E., T.J. Fielding, E.J. Wright, R. Walker, B.E. Parsons and S. Hensley (2006). Displacement field and slip distribution of the 2005 Kashmir earthquake from SAR imagery, Geophys. Res. Lett., 33, L20310; doi: 10.1029/2006GL027193.

Pulinets, S.A. (1998). Seismic activity as a source of the ionospheric variability, Adv. Space Res., 22, 903-906; doi: 10.1016/S0273-1177(98)00121-5.

Pulinets, S.A., A.D. Legen'ka, T.V. Gaivoronskaya and V.K. Depuev (2003). Main phenomenological features of ionospheric precursors of strong earthquakes, J. Atmos. Sol.-Terr. Phys., 65 (b), 1337-1347.

Shvets, A.V., M. Hayakawa and O.A. Molchanov (2002). Subionospheric VLF monitoring for earthquake-related ionospheric perturbations, J. Atmos. Electricity, 22, 87-99.

Singh, S.K., A. Iglesias, R.S. Dattatrayam, B.K. Bansal, S.S. Rai, X. Perez-Campos, G. Suresh, P.R. Baidya and J.L. Gautam (2006). Muzaffarabad earthquake of 8 October, 2006 (Mw 7.6): a preliminary report on source characteristics and recorded ground motion, Current Science, 91, 689-695.

Takeo, Y., I. Tomizawa and T. Sugimoto (1992). Results of statistical analysis of LF seismogenic emissions as precursors to the earthquake and volcanic eruptions, Res. Lett. Atmos. Electr., 12, 203-210.

Thomson, N.R. and M.A. Clilverd (2001). Solar-flare-induced ionospheric D-region enhancements from VLF amplitude observations, J. Atmos. Sol.- Terr. Phys., 63, 1729-1737.

Sarkar, S.K. and B.K. De (1985). Ionospheric effect of Leonid meteor shower at 70 km height, Annales Geophysicae, 3, 113-118.

Sarkar, S.K. and B.K. De (1991). Characteristics of seasonal variation of fadings of atmospherics associated with geomagnetic activity, Annales Geophysicae, 9, 597-602.

Yoshino, T. and I. Tomizawa (1989). Observation of low-frequency electromagnetic emissions as precursors to the volcanic eruption at Mt. Mihara during November, 1986, Phys. Earth Planet. Int., 57, 32-39.

*Corresponding author: Syam Sundar De,
S. K. Mitra Centre for Research in Space Environment,
Institute of Radio Physics and Electronics, University of Calcutta,
Kolkata, India; email: de_syam_sundar@yahoo.co.in.